Letters in Drug Design & Discovery, 2021, *18*, 372-386

RESEARCH ARTICLE

Design and Efficient Synthesis of Novel 4,5-Dimethylthiazole-Hydrazone Derivatives and their Anticancer Activity

Asaf Evrim Evren[1,2,*], Leyla Yurttaş[1], Büşra Ekselli[3], Onur Aksoy[3] and Gülşen Akalin-Çiftçi[3]

[1]*Department of Pharmaceutical Chemistry, Faculty of Pharmacy, Anadolu University, Eskişehir, Turkey;* [2]*Pharmacy Services, Vocational School of Health Services, Bilecik Şeyh Edebali University, Bilecik, Turkey;* [3]*Department of Biochemistry, Faculty of Pharmacy, Anadolu University, Eskişehir, Turkey*

ARTICLE HISTORY

Received: June 17, 2020
Revised: September 13, 2020
Accepted: September 28, 2020

DOI:
10.2174/1570180817999201022192937

Abstract: ***Background*:** Recently, researchers have been warning about the increased mortality of the various cancer types. Also, the lung adenocarcinoma and the glioma types are burning issues for world's health due to late or wrong diagnosis and/or insufficient treatment methods. For this purpose, our research group designed and synthesized novel 4,5-dimethyl thiazole-hydrazone derivatives which were tested against cancer and normal cell lines to understand the structure-activity relationship (SAR).

***Methods*:** The lead compounds were obtained by reacting 2-(substituted aryl-2-ylmethylene) hydrazin-1-carbothioamide with 3-chloro-2-butanone derivatives. The structural elucidation of the compounds was performed by ^{1}H-NMR, ^{13}C-NMR, and LC/MS-IT-TOF spectral and elemental analyses. The synthesized compounds were tested *in vitro* for the anticancer activity against A549 human lung adenocarcinoma and C6 rat glioma cells and investigated for which pathway to induce cell death. Also, the docking study of the active compounds was achieved to understand the SAR.

***Results*:** The targeted compounds (**2a-2l**) were synthesized successfully above 70% yields, and the analysis findings proved their purity. In general, the results of activity studies displayed significant effects against at least one cell line, except compounds **2e** (indol-3-yl) and **2h** (4-dimethylaminophenyl). Furthermore, compounds **2b** and **2f** displayed potential anticancer activity. With the help of molecular docking study, a potential selectivity of compound **2f** was observed for type II protein kinase. On the other hand, compound **2b** interacted with the active site nearly the same as Dasatinib. Therefore, these two compounds could be used as a base on developing selective anticancer drugs.

***Conclusion*:** Pyridin-2-yl (**2b**) derivative was found to be a favorable molecule with high anticancer potency against C6 and A549 cell lines. Additionally, 1-naphthyl (**2f**) derivative was a worthy compound for potential selectivity. In future studies, it will be our priority to focus on developing derivatives of these two compounds (**2b** and **2f**) and elucidate their mechanisms.

Keywords: Thiazole, hydrazone, A549, C6, apoptosis, anticancer activity.

1. INTRODUCTION

The uncontrolled cell division in one or more organs or tissues is described as cancer [1, 2]. Recently, researchers have warned about the increased mortality of the various cancer types [3]. Also, the lung adenocarcinoma and the glioma types are burning issues for world's health [4-6] due to late or wrong diagnosis [7] and/or insufficient treatment methods [8-10]. Today, some pharmacological options are used against tumor cells such as surgical operation, chemotherapy, and radiation therapy. There are no methods or viable techniques for the radical treatment yet, especially for the last stage of these types [11, 12]. Another major challenge that complicates the struggle against tumor cells is drug resistance as reported by several studies [13-15]. Since these difficulties terrorize humanity, researchers focus on new therapy procedures [16-19] and/or new diagnosis techniques [20-22] for cancer treatment. According to literature, synthesis of new drug agents [23-25], and discovering or illuminating new pathways [26, 27] are substantially preferred techniques in the combat against cancer.

The thiazole ring has an important position in medicinal chemistry because it is a small structure, and it shows different biological activities by acting in diverse pathways

*Address correspondence to this author at the Department of Pharmaceutical Chemistry, Faculty of Pharmacy, Anadolu University, Eskişehir, Turkey and Pharmacy Services, Vocational School of Health Services, Bilecik Şeyh Edebali University, Bilecik, Turkey;
E-mail: asafevrimevren@anadolu.edu.tr

1875-628X/21 $65.00+.00

[28, 29]. Over the past decade, thiazole moiety has displayed analgesic [30], antimicrobial [31] and peripheral antinociceptive [32] activities. Likewise, its anticancer activity studies are increasing day by day [33-35]. Thiazole derivatives, tiazofurin [36], and dasatinib [37, 38] are currently used for their cytotoxicity effect clinically. Similarly, hydrazone moiety possessing an azomethine proton constitutes an important class of compounds for new drug design and development [39]. A previous histone acetyltransferases (HAT) enzyme study displayed that good anticancer activity of synthesized compounds has been associated with (thiazole-2-yl) hydrazone moiety [40]. On the other hand, nitrogen-containing heterocyclic rings like pyridine, pyrrole, and indole have various biological activities [41-45]. Literature reviews denoted those pyridine derivatives have a good anticancer profile [46, 47]. Furthermore, thiazole bearing pyridine derivatives have been reported for their anticancer activity [48, 49]. Hence, it led us to the hybridization of these three moieties.

Based on the above information, we synthesized and analyzed new twelve 4,5-dimethyl-thiazole-2-hydrazone derivatives (**2a-2l**), and then evaluated the anticancer activity against C6 rat glioma cells and A549 human lung carcinoma cells. Additionally, we tested their cytotoxicity against NIH3T3 murine fibroblast and L929 mouse fibroblast cell lines.

2. EXPERIMENTAL

2.1. Chemistry

All chemicals used in the synthesis were purchased either from Merck Chemicals (Merck KGaA, Darmstadt, Germany) or Sigma-Aldrich Chemicals (Sigma-Aldrich Corp., St. Louis, MO, USA). The reactions and the purities of the compounds were observed by thin-layer chromatography (TLC) on silica gel 60 F254 aluminum sheets obtained from Merck (Darmstadt, Germany). Melting points of the synthesized compounds were recorded by the MP90 digital melting point apparatus (Mettler Toledo, Ohio, USA) and presented as uncorrected. ^{1}H NMR and ^{13}C NMR spectral analyses were achieved using a Bruker 300 MHz and 75 MHz digital FT-NMR spectrometer (Bruker Bioscience, Billerica, MA, USA) in DMSO-d_6. In the NMR spectra, splitting patterns were designated as follows: s: singlet; d: doublet; t: triplet; m: multiplet. Coupling constants (*J*) were reported as Hertz. High resolution mass spectrometric (HRMS) analysis was performed using a LC/MS-IT-TOF system (Shimadzu, Kyoto, Japan). Elemental analysis was performed on a Leco 932 CHNS analyzer (Leco, Michigan, USA).

2.1.1. General procedure for the synthesis of the compounds 2-(substituted aril-2-ylmethylene)hydrazine-1-carbothioamide derivatives (1a-1l)

Thiosemicarbazide (1 eq.) and aldehyde derivatives (1 eq.) were dissolved in ethanol. The mixture was refluxed for 2 h at 200 ºC. We used TLC to understand the completion of the reaction. Compounds **1a, 1b** [50], **1c** [51], **1d** [52], **1e** [53], **1f** [54], **1g** [55], **1h** [56], **1i** [54], **1j** [56], **1k** [57] and **1l** [54] were described previously.

2.1.2. 4,5-Dimethyl-2-(2-(arylmethylene)hydrazinyl)thiazole derivatives (2a-2l)

A mixture of 2-(substituted aryl-2-ylmethylene)hydrazin-1-carbothioamide derivatives (**1a-1l**) (1 eq.) and 3-chloro-2-butanone (1 eq.) in ethanol was stirred for 6 h at room temperature. The solvent was then evaporated to dryness. The final compounds were recrystallized from ethanol.

2.1.3. 4,5-Dimethyl-2-[2-(pyridin-4-ylmethylene)hydrazinyl] thiazole (2a, $C_{11}H_{12}N_4S$)

M. p. 248ºC, 85%, orange powder, ^{1}H-NMR (300 MHz, DMSO-d_6, ppm) δ 2.09 (s, 3H, CH_3), 2.18 (s, 3H, CH_3), 7.97 (d, 2H, *J*=6.74 Hz, Ar-H), 8.12 (s, H, N=C-H), 8.73 (d, 2H, *J*=6.72 Hz, Ar-H), 9.27 (brs, H, N-H). ^{13}C-NMR (75 MHz, DMSO-d_6, ppm) δ 11.38 (CH_3), 13.74 (CH_3), 119.15, 122.31, 137.36, 142.76 (C=N), 150.43, 156.57. For $C_{11}H_{12}N_4S$ elemental Analysis results for C, H, and N calculated: 56.87%, 5.21%, and 24.12%; found: 56.90%, 5.17%, and 24.07%. HRMS (m/z): $[M+1]^+$ calculated 233.0855; found 233.0862.

2.1.4. 4,5-Dimethyl-2-[2-(pyridin-2-ylmethylene)hydrazinyl]thiazole (2b, $C_{11}H_{12}N_4S$) [58]

M. p. 202ºC, 72%, dusty rose powder, ^{1}H-NMR (300 MHz, $CDCl_3$, ppm) δ 2.21 (s, 3H, CH_3), 2.25 (s, 3H, CH_3), 7.29-7.34 (m, H, Ar-H), 7.83-7.87 (m, 2H, Ar-H), 8.05 (s, H, N=C-H), 8.62 (d, H, *J*=5.10 Hz, Ar-H), 9.26 (brs, H, N-H). ^{13}C-NMR (75 MHz, DMSO-d_6, ppm) δ 11.25 (CH_3), 13.64 (CH_3), 121.27, 124.70, 126.43, 139.54, 139.98, 140.54 (C=N), 146.80, 147.69, 151.50. For $C_{11}H_{12}N_4S$ elemental Analysis results for C, H, and N calculated: 56.87%, 5.21%, and 24.12%; found: 56.91%, 5.16%, and 24.16%. HRMS (m/z): $[M+1]^+$ calculated 233.0855; found 233.0853.

2.1.5. 2-[2-[(1H-pyrrol-2-yl)methylene]hydrazinyl]-4,5-dimethylthiazole (2c, $C_{10}H_{12}N_4S$)

M. p. 240ºC, 75%, navy blue powder, ^{1}H-NMR (300 MHz, DMSO-d_6, ppm) δ 2.18 (s, 3H, CH_3), 2.22 (s, 3H, CH_3), 6.13-6.16 (m, H, Ar-H), 6.56 (brd, *J*=1.13 Hz, H, Ar-H), 7.02 (s, H, Ar-H), 8.21 (s, H, N=C-H), 11.30 (brs, H, pyrole N-H), 11.95 (brs, H, N-H). ^{13}C-NMR (75 MHz, DMSO-d_6, ppm) δ 10.98 (CH_3), 11.89 (CH_3), 110.09, 113.53, 114.62, 123.64, 127.07, 132.25 (C=N), 140.59. For $C_{10}H_{12}N_4S$ elemental Analysis results for C, H, and N calculated: 54.52%, 5.49%, and 25.43%; found: 54.53%, 5.48%, and 25.42%. HRMS (m/z): $[M+1]^+$ calculated 221.0855; found 221.0847.

2.1.6. 4,5-Dimethyl-2-[2-[(1-methyl-1H-pyrrol-2-yl)methylene]hydrazinyl] thiazole (2d, $C_{11}H_{14}N_4S$)

M. p. 187ºC, 80%, off-white solid, ^{1}H-NMR (300 MHz, DMSO-d_6, ppm) δ 2.16 (s, 3H, CH_3), 2.18 (s, 3H, CH_3), 3.84 (s, 3H, pyrrol-CH_3), 6.12-6.14 (m, H, Ar-H), 6.59-6.60 (m, H, Ar-H), 7.06 (brt, H, *J*=1.39, Ar-H), 8.39 (s, H, N=C-H), 12.11 (brs, H, N-H). ^{13}C-NMR (75 MHz, DMSO-d_6, ppm) 10.97 (CH_3), 12.20 (CH_3), 36.91 (CH_3), 109.17, 113.85, 117.00, 126.39, 129.92, 133.39 (C=N), 142.23. For $C_{11}H_{14}N_4S$ elemental Analysis results for C, H, and N calculated: 56.38%, 6.02%, and 23.91%; found: 56.41%,

5.58%, and 23.90%. HRMS (m/z): $[M+1]^+$ calculated 235.1012; found 235.1001.

2.1.7. 2-[2-[(1H-indol-3-yl)methylene]hydrazinyl]-4,5-dimethylthiazole (2e, $C_{14}H_{14}N_4S$)

M. p. 204°C, 81%, cream solid, ^{1}H-NMR (300 MHz, DMSO-d_6, ppm) δ 2.18 (s, 3H, CH_3), 2.21 (s, 3H, CH_3), 7.18-7.26 (m, 2H, Ar-H), 7.49 (d, H, *J*=7.38 Hz, Ar-H), 7.95 (d, *J*=2.75 Hz, H, Ar-H), 8.16 (d, H, *J*=7.15 Hz, Ar-H), 8.68 (s, H, N=C-H), 11.28 (brs, H, indole N-H), 11.92 (brs, H, N-H). ^{13}C-NMR (75 MHz, DMSO-d_6, ppm) δ 11.00 (CH_3), 12.13 (CH_3), 110.93, 112.65, 113.59, 121.49, 122.12, 123.42, 124.28, 133.01, 137.67, 147.13 (C=N), 165.19. For $C_{14}H_{14}N_4S$ elemental Analysis results for C, H, and N calculated: 62.20%, 5.22%, and 20.72%; found: 62.26%, 5.18%, and 20.65%. HRMS (m/z): $[M+1]^+$ calculated 271.1012; found 271.0999.

2.1.8. 4,5-Dimethyl-2-[2-(naphthalen-1-ylmethylene)hydrazinyl]thiazole (2f, $C_{16}H_{15}N_3S$)

M. p. 216°C, 83%, burnt orange solid, ^{1}H-NMR (300 MHz, DMSO-d_6, ppm) δ 2.17 (s, 3H, CH_3), 2.18 (s, 3H, CH_3), 7.59-7.63 (m, 2H, Ar-H), 7.65-7.71 (m, H, Ar-H), 8.00-8.07 (m, 3H, Ar-H), 8.57 (d, H, *J*=8.39 Hz, Ar-H), 9.25 (brs, H, N=C-H), 11.95 (brs, H, N-H). ^{13}C-NMR (75 MHz, DMSO-d_6, ppm) 10.99 (CH_3), 12.18 (CH_3), 114.70, 123.96, 126.01, 126.87, 128.08, 128.81, 129.41, 130.58, 131.75, 133.68, 133.94, 148.61 (C=N), 165.51. For $C_{16}H_{15}N_3S$ elemental Analysis results for C, H, and N calculated: 68.30%, 5.37%, and 14.93%; found: 68.39%, 5.33%, and 14.88%. HRMS (m/z): $[M+1]^+$ calculated 282.1059; found 282.1045.

2.1.9. 4,5-Dimethyl-2-[2-(naphthalen-2-ylmethylene)hydrazinyl]thiazole (2g, $C_{16}H_{15}N_3S$)

M. p. 233°C, 76%, yellow powder, ^{1}H-NMR (300 MHz, $CDCl_3$, ppm) δ 2.27 (s, 3H, CH_3), 2.28 (s, 3H, CH_3), 7.28 (s, H, Ar-H), 7.55-7.58 (m, 2H, Ar-H), 7.85-7.91 (m, 3H, Ar-H), 7.99 (s, H, Ar-H), 8.43 (s, H, N=C-H), 11.96 (brs, H, N-H). ^{13}C-NMR (75 MHz, DMSO-d_6, ppm) δ 10.98 (CH_3), 12.20 (CH_3), 114.71, 122.86, 127.37, 127.97, 128.28, 128.93, 129.01, 130.20, 131.33, 133.20, 134.42, 148.86 (C=N), 165.12. For $C_{16}H_{15}N_3S$ elemental Analysis results for C, H, and N calculated: 68.30%, 5.37%, and 14.93%; found: 68.26%, 5.41%, and 14.91%. HRMS (m/z): $[M+1]^+$ calculated 282.1059; found 282.1045.

2.1.10. 4-[[2-(4,5-Dimethylthiazol-2-yl)hydrazinylidene]methyl]-N,N-dimethylaniline (2h, $C_{14}H_{18}N_4S$)

M. p. 89-91°C, 79%, yellow solid, ^{1}H-NMR (300 MHz, DMSO-d_6, ppm) δ 2.18 (s, 3H, CH_3), 2.99 (s, 3H, CH_3), 3.03 (s, 6H, N-CH_3), 6.78 (d, *J*=8.88 Hz, 2H, Ar-H), 7.68 (d, *J*=8.93 Hz, 2H, Ar-H), 9.66 (s, H, N=C-H), 11.82 (brs, H, N-H). ^{13}C-NMR (75 MHz, DMSO-d_6, ppm) 10.95 (CH_3), 11.98 (CH_3), 40.13 (CH_3), 40.76 (CH_3), 111.56, 113.18, 125.02, 129.50, 131.98, 150.04 (C=N), 151.71, 154.62, 190.30. For $C_{14}H_{18}N_4S$ elemental Analysis results for C, H, and N calculated: 61.28%, 6.61%, and 20.42%; found: 61.32%, 6.58%, and 20.45%. HRMS (m/z): $[M+1]^+$ calculated 275.1325; found 275.1316.

2.1.11. 4,5-Dimethyl-2-[2-[4-(trifluoromethyl)benzylidene]hydrazinyl]thiazole (2i, $C_{13}H_{12}F_3N_3S$)

M. p. 215-220°C, 71%, yellow powder, ^{1}H-NMR (300 MHz, DMSO-d_6, ppm) δ 2.18 (s, 6H, CH_3), 7.78 (d, *J*=8.25 Hz, 2H, Ar-H), 7.99 (d, *J*=8.07 Hz, 2H, Ar-H), 8.51 (s, H, N=C-H), 11.46 (brs, H, N-H). ^{13}C-NMR (75 MHz, DMSO-d_6, ppm) δ 10.94 (CH_3), 12.11 (CH_3), 115.19, 126.07, 126.12, 127.31, 128.44, 133.58, 141.18 (C=N), 147.08, 165.21. For $C_{13}H_{12}F_3N_3S$ elemental Analysis results for C, H, and N calculated: 52.17%, 4.04%, and 14.04%; found: 52.20%, 4.01%, and 14.08%. HRMS (m/z): $[M+1]^+$ calculated 300.0732; found 300.0732.

2.1.12. 2-[[2-(4,5-Dimethylthiazol-2-yl)hydrazinyliden]methyl]phenol (2j, $C_{12}H_{13}N_3OS$)

M. p. 233°C, 80%, light yellow powder, ^{1}H-NMR (300 MHz, DMSO-d_6, ppm) δ 2.17 (s, 3H, CH_3), 2.19 (s, 3H, CH_3), 6.88 (t, *J*=7.46 Hz, H, Ar-H), 6.98 (d, *J*=8.37 Hz, H, Ar-H), 7.25-7.31 (m, H, Ar-H), 7.77 (d, *J*=7.44 Hz, H, Ar-H), 8.66 (s, H, N=C-H), 10.41 (brs, H, OH), 12.51 (brs, H, N-H). ^{13}C-NMR (75 MHz, DMSO-d_6, ppm) δ 11.02 (CH_3), 12.18 (CH_3), 113.84, 116.85, 119.70, 119.80, 127.03, 132.50, 133.27, 146.25 (C=N), 157.47, 165.10. For $C_{12}H_{13}N_3OS$ elemental Analysis results for C, H, and N calculated: 58.28%, 5.30%, and 16.99%; found: 58.23%, 5.34%, and 17.01%. HRMS (m/z): $[M+1]^+$ calculated 248.0852; found 248.0842.

2.1.13. 4,5-Dimethyl-2-[2-(3,4,5-trimethoxybenzyliden)hydrazinyl]thiazole (2k, $C_{15}H_{19}N_3O_3S$)

M. p. 214-217°C, 79%, white powder, ^{1}H-NMR (300 MHz, DMSO-d_6, ppm) δ 2.19 (s, 6H, CH_3), 3.70 (s, 3H, OCH_3), 3.84 (s, 6H, OCH_3), 7.14 (s, 2H, Ar-H), 8.34 (s, H, N=C-H), 12.00 (brs, H, N-H). ^{13}C-NMR (75 MHz, DMSO-d_6, ppm) δ 11.02 (CH_3), 12.31 (CH_3), 56.57 (O-CH_3), 60.62 (O-CH_3), 105.36, 114.51, 129.09, 133.81, 140.24, 148.51 (C=N), 153.67, 165.00. For $C_{15}H_{19}N_3O_3S$ elemental Analysis results for C, H, and N calculated: 56.06%, 5.96%, and 13.07%; found: 56.10%, 5.91%, and 13.09%. HRMS (m/z): $[M+1]^+$ calculated 322.1220; found 322.1216.

2.1.14. 2-[2-(4-Isopropylbenzyliden)hydrazinyl]-4,5-dimethylthiazole (2l, $C_{15}H_{19}N_3S$)

M. p. 70°C, 70%, white solid, ^{1}H-NMR (300 MHz, DMSO-d_6, ppm) δ 1.20 (q, J_1=2.54 Hz, J_2=6.84 Hz, 6H, *i*-propyl CH_3), 2.18 (s, 6H, CH_3), 2.86-3.00 (m, H, CH), 7.33 (d, *J*=8.05 Hz, 2H, Ar-H), 7.70 (d, *J*=8 Hz, 2H, Ar-H), 8.44 (s, H, N=C-H), 11.98 (brs, H, N-H). ^{13}C-NMR (75 MHz, DMSO-d_6, ppm) δ 10.96 (CH_3), 12.09 (CH_3), 23.88 (CH_3), 24.04 (CH_3), 33.89 (CH), 114.54, 127.32, 128.05, 130.19, 131.25, 149.20 (C=N), 152.02, 193.06. For $C_{15}H_{19}N_3S$ elemental Analysis results for C, H, and N calculated: 65.90%, 7.01%, and 15.37%; found: 65.87%, 7.05%, and 15.34%. HRMS (m/z): $[M+1]^+$ calculated 274.1372; found 274.1370.

2.2. Biochemistry

2.2.1. Model Cell Line

The A549 (human lung adenocarcinoma) and C6 (rat glioma) NIH3T3, (murine fibroblast), and L929 (the mouse

fibroblast) (ATCC, Rockville, MD, USA) cells were maintained in 75 cm^2 sterile plastic tissue culture flasks in 90% RPMI or DMEM (Sigma, Deisenhofen, Germany) medium supplemented with 10% (v/v) FBS (Gibco, Paisley, UK), and penicillin/streptomycin (Gibco, Paisley, UK) (100 units/mL) as adherent monolayers. These cells were grown at 37°C in a humidified atmosphere containing 5% CO_2 in air. The methods were carried out as previously described [59].

2.2.2. Cell Culture and Cytotoxicity Analysis

MTT (3-(4,5-dimethylthiazol-2-yl)-2,5-diphenyltetrazolium bromide) method was performed to measure the cytotoxicity of the tested compounds against C6, A549, L929 and NIH3T3 cell lines according to the reported data. NIH3T3, L929 were harvested and cultured at 37°C in a humidified atmosphere of 95% air and 5% CO2 in Dulbecco's modified eagle's medium (DMEM, Sigma, St Louis, MO, USA). A549 and C6 cells were harvested and cultured at 37°C in a humidified atmosphere of 95% air and 5% CO2 in RPMI. Four cell lines growth mediums were also supplemented with 5% fetal calf serum (FCS) (Sigma-Aldrich, St Louis, MO, USA), and penicillin (50 IU /mL) and streptomycin (50 µg/mL) solution. Subcultivation was performed with cells from confluent cultures treated with 0.5 g/L- 0.2 g/L ethylenediaminetetraacetic acid in phosphate-buffered saline (PBS). L929 and NIH3T3 cells were diluted in fresh medium and seeded into 96-well plates as $2x10^4$ cells per well. On the other hand, A549 and C6 cells were cultured at a density of 5×10^3 cells per well in flat bottomed 96-well plates. All of the synthesized compounds and control drugs (mitoxantrone and cisplatin) were dissolved in DMSO. Further dilutions were made by their own growth medium (DMEM for L929 and NIH/3T3 or RPMI for C6 and A549) (Final DMSO concentration was <0.1% which has no effect on the viability of cells). Also, control cells were untreated [60-64]. These prepared compounds were administered to cells in 1.95-1000 µM range. After 24 h incubation time, the MTT (Sigma-Aldrich, St. Louis, MO, USA) powder (5 mg/mL) dissolved in phosphate-buffered saline (PBS) (Gibco, Paisley, UK) was added to each well (20 µL). After a 2-4 h period in the same conditions, the medium was removed from the plate and 100 µL of DMSO was added to each well to dissolve the dye and kept for 10 minutes. Purple formazan was generated at the end of the process which is the reduction product of the MTT agent by the mitochondrial dehydrogenase enzyme of intact cells. The cells were measured at 540 nm using a microtiter plate reader (BioTek Plate Reader, Winooski, VT, USA). Cell viability was calculated as a percent ratio and compared with the control cells. Each concentration was repeated in three wells and half-maximal inhibitory concentration 50 (IC_{50}) values were defined as the drug concentrations that reduced absorbance to 50% of control values by using logarithmic graphics. The percentage of the viable cells was calculated based on the medium control using the following formula:

$$(\%) = [100 \times (\text{sample abs})/ (\text{control abs})$$

2.2.3. The Determination of Early/late Apoptosis by Flow Cytometry

After the A549 and C6 cells were incubated with the most potent antiproliferative agents in this series at IC_{50} concentrations, phosphatidylserine externalization, which indicates early apoptosis, was measured by the FITC Annexin V apoptosis detection kit (BD Pharmingen, San Jose, CA, USA) on a BD FACSAria flow cytometer for 24 h. The A549 and C6 cells were harvested and washed twice with ice-cold PBS and resuspended in 100 µL of binding buffer. A volume of 5 µL (5 µg/mL) of Annexin V-FITC and PI were added to the cells and incubated for 15 min in the dark at room temperature (20-25°C). Then, 400 µL of binding buffer was added to the mixture samples and analyzed on a BD FACSAria flow cytometer using FACSDiva version 6.1.1 software (BD Biosciences, San Jose, CA, USA).

2.2.4. Prediction of the ADME Properties

The prediction of the physicochemical parameters of compounds (**2a-2l**) was calculated using the SwissADME web-based program [65-67].

2.2.5. Molecular Docking Study

Crystal structure of protein kinase enzyme was retrieved from Protein Data Bank server (PDB code: 4YBJ). Protein preparation process, ligand preparation process, grid generation, docking and visualization studies were worked on Schrodinger's Maestro molecular modeling package [68].

The water molecules were removed from the crystal structure. Ligands were set to the physiological pH (pH = 7.4) at the protonation step. In molecular docking simulations: Glide/XP docking protocols were applied for the prediction of topologies of **2b**, **2f** and dasatinib at the active site of target structure [69]. After the preparation steps they were docked to the active site of 4YBJ. The docking study was used here to predict the relationship between structure and inhibition of protein kinase enzyme.

3. RESULTS

3.1. Chemistry

In this study, we synthesized twelve new *N*-(5-methyl-4-phenylthiazol-2-yl)acetamide derivatives. The synthesis reaction was performed via two steps. In the first step, thiosemicarbazide and aryl aldehyde derivatives were reacted in ethanol to get 2-(arylmethylene)hydrazine-1-carbothioamide. The intermediate products (**1a-1l**) and 3-chloro-butan-2-one were reacted for ring closure to obtain the final compounds (**2a-2l**) as shown in Scheme **1**. All the synthesized compounds were characterized by analytical and spectral data.

The ^{1}H-NMR spectra of compounds showed signals at δ 2.09-2.99 ppm for methyl (CH_3) protons which were singlet peaks. Methylene (C-H) protons were observed at δ 8.05-9.66 ppm as a single peak and a broad singlet peak seen at δ 9.26-12.51 ppm indicated the hydrazone N-H proton. The appearance of singlet, doublet, triplet and/or multiplets peaks at δ 6.12-8.62 ppm were due to the aromatic protons. The

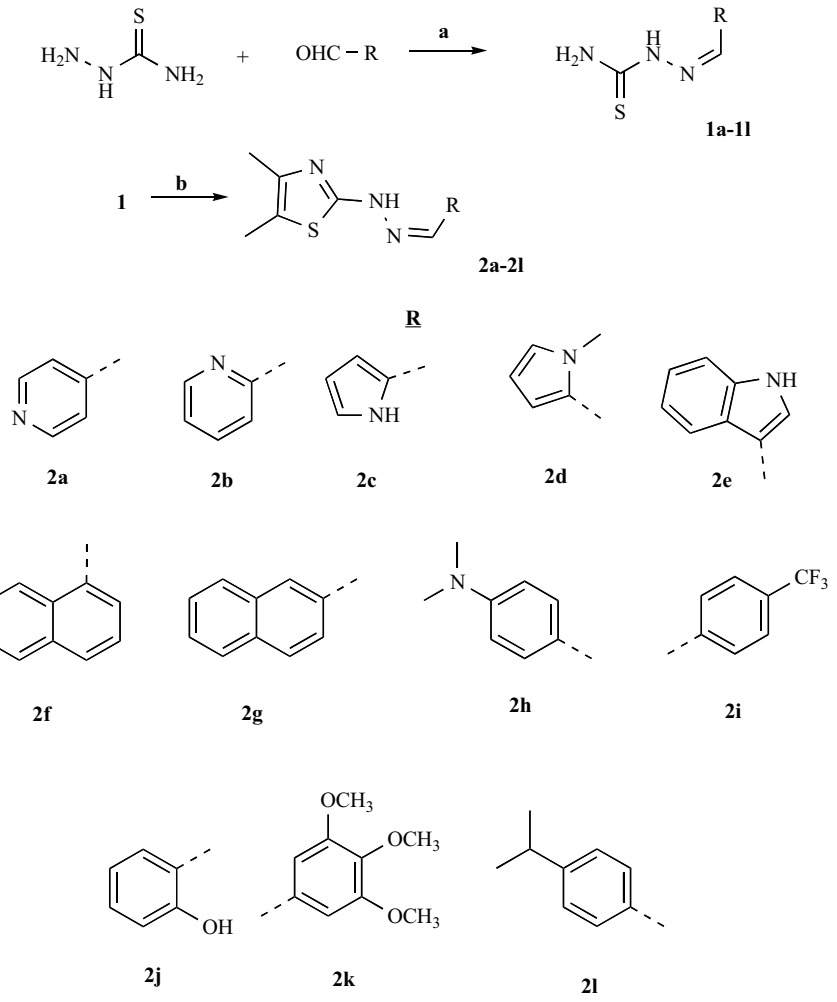

Reaction and conditions: **a)** EtOH, reflux, **b)** 3-Chlorobutan-2-one, EtOH, rt.

Scheme 1. The reaction route of the compounds.

^{13}C-NMR spectra of compounds showed signals at δ 10.94-13.74 ppm for methyl (CH_3) carbon, at δ 105.36-193.06 ppm for aromatic carbons and δ 132.25-150.04 ppm for hydrazone (N-N=C) carbon. All masses were estimated by the M+H values. Elemental analysis results for C, H, and N agreed with the calculated values for the synthesized compounds.

3.2. Anticancer Activity

The cytotoxicity assays and determination of IC_{50} doses of cisplatin, mitoxantrone and synthesized compounds against A549, C6, NIH3T3, and L929 cells were performed by MTT assay and the results were shown in Table **1**. Relating to the assay results, compounds **2a**, **2b** and **2l** displayed anticancer activity against both tumor cell types. Compounds **2g**, **2i, 2j** and **2k** showed inhibitory activity only against lung cancer, and compounds **2c**, **2d** and **2f** presented only anti-glioma activity. On the other hand, compounds **2e** and **2h** did not exhibit anticancer activity against both tumor cell types. Also, compounds **2a**, **2g,** and **2l** were found cytotoxic on NIH3T3 or L929 cells at therapeutic doses against A549 cells and only **2h** displayed cytotoxicity on NIH3T3 or L929 cells at its therapeutic dose against both cancer types.

Compound **2b** (R: pyridin-2-yl) and **2f** (R: 1-naphthyl) displayed strong activity against the C6 cell line. Compound **2b** (IC_{50}: <16.79 μM) and **2f** (IC_{50}: 22.21±2.67 μM) were more active than cisplatin (IC_{50}: 32.44±5.97 μM) yet rest of the compounds were less active than cisplatin against C6 cancer cells. None of the compounds showed powerful activity than mitoxantrone against the C6 cell line. Only compound **2b** (IC_{50}: <16.79 μM) was more active than mitoxantrone against A549 cells (IC_{50}: 19.50±5.67 μM).

According to IC_{50} values, the apoptotic effects of compounds and mitoxantrone were analyzed for A549 human lung adenocarcinoma and C6 rat glioma cells based on Annexin V-PI binding capacities in flow cytometry as shown in (Figs. **1** and **2**).

Compound **2b** (total apoptotic rate: 44%) showed a considerably high apoptotic effect and minimal necrosis effect (Necrosis Rate: 0.1%) on C6 cells. Also, when **2b** was compared with mitoxantrone, almost the same apoptotic rate and extremely low necrotic effect at their IC_{50} doses was

Table 1. IC_{50} value of the compounds against A549, C6, NIH/3T3, and L929 cell lines.

-	Cell Lines	Average IC_{50}	Compounds	Cell Lines	Average IC_{50}
2a	A549	398.18±15.24	**2g**	A549	402.77±41.05
	C6	51.66±7.08		C6	>1000
	3T3	>1000		3T3	44.31±2.48
	L929	109.40±9.10		L929	22.19±1.42
2b	A549	<16.79	**2h**	A549	>1000
	C6	<16.79		C6	>1000
	3T3	>1000		3T3	217.46±35.51
	L929	>1000		L929	416.75±46.71
2c	A549	>1000	**2i**	A549	85.76±13.50
	C6	83.98±15.89		C6	>1000
	3T3	>1000		3T3	>1000
	L929	>1000		L929	>1000
2d	A549	>1000	**2j**	A549	95.69±15.32
	C6	51.21±8.54		C6	>1000
	3T3	>1000		3T3	>1000
	L929	>1000		L929	>1000
2e	A549	>1000	**2k**	A549	121.34±4.39
	C6	>1000		C6	>1000
	3T3	>1000		3T3	>1000
	L929	>1000		L929	>1000
2f	A549	>1000	**2l**	A549	130.46±14.78
	C6	22.21±2.67		C6	41.44±1.72
	3T3	>1000		3T3	35.86±3.79
	L929	>1000		L929	98.49±12.62
Mitoxantrone	A549	19.50±5.67	**Cisplatin**	A549	n.t.
	C6	8.77±0.32		C6	32.44±5.97
	3T3	n.t.		3T3	n.t.
	L929	n.t.		L929	n.t.

The unit of value is μM and there it is represented as the average of three replicates. n.t.: not tested.

determined. On the other hand, **2f** killed 49.7% of the cells; it stated the necrotic effect as 19.3% and apoptotic rate as 30.4%. When considering the apoptosis rate and IC_{50} doses together, **2b** was better than **2f** and mitoxantrone due to the lowest necrosis rate. Even though compounds **2a**, **2c** and **2l** have low necrosis rate than mitoxantrone, their anticancer activity was not enough against C6 cells. In relation to the apoptotic rates of A549 cell lines, only compound **2b** was

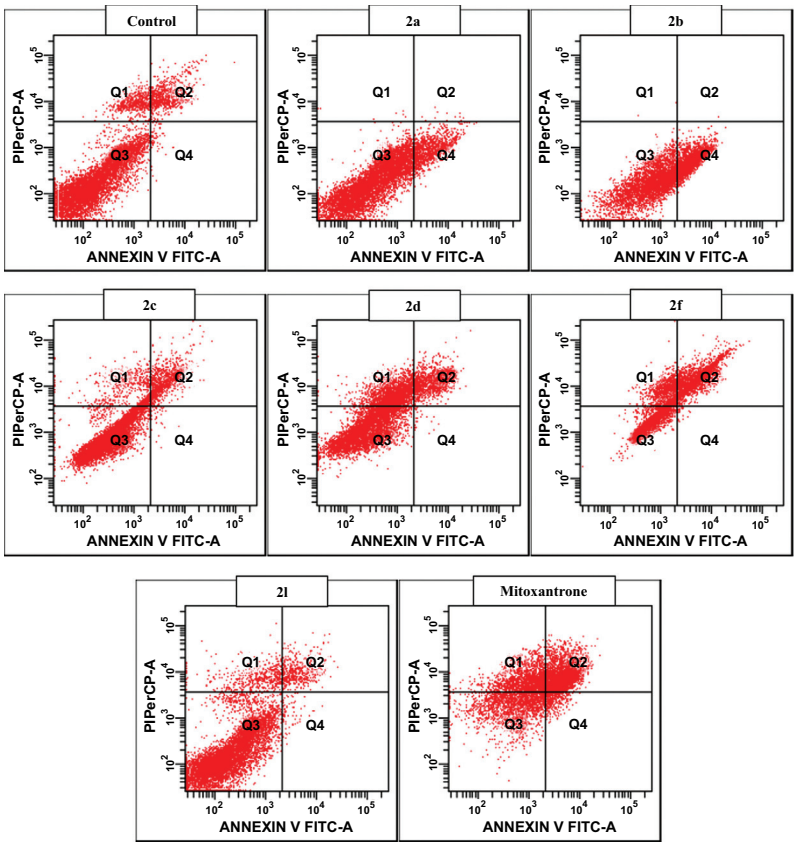

Fig. (1). Flow cytometric analysis of C6 cells treated with IC50 values of compounds **2a, 2b, 2c, 2d, 2f, 2l,** and mitoxantrone. (*A higher resolution / colour version of this figure is available in the electronic copy of the article*).

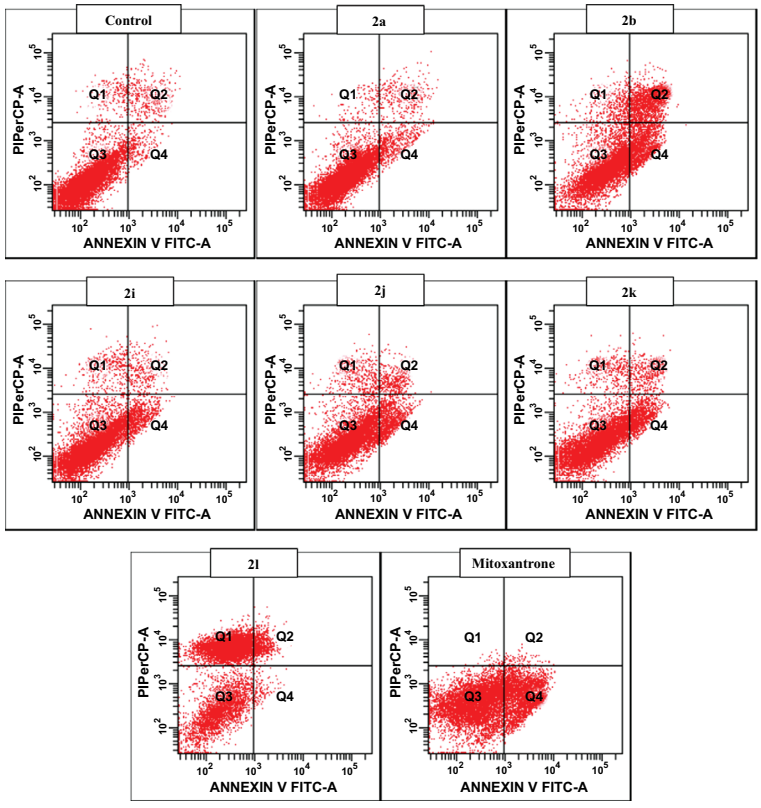

Fig. (2). Flow cytometric analysis of A549 cells treated with IC50 values of compounds **2a, 2b, 2i, 2j, 2k, 2l,** and mitoxantrone. (*A higher resolution / colour version of this figure is available in the electronic copy of the article*).

Table 2. Apoptotic rates of compounds on C6 cell lines (%).

-	Early Apoptotic Cells	Late Apoptotic Cells	Total Apoptotic Cells	Necrosis Cells	Viable Cells
Control	0.4	8.5	8.9	7.1	84.0
2a	13.4	0.1	13.5	0.1	86.4
2b	44.4	0.0	44.4	0.1	55.5
2c	0.4	9.6	10.0	8.0	82.0
2d	0.3	11.9	12.2	26.8	61.0
2f	0.3	30.1	30.4	19.3	50.3
2l	0.8	5.1	5.9	5.6	88.5
R.F.	5.1	50.2	55.3	21.8	22.9

R.F: Reference drug (Mitoxantrone). (C6 cells were cultured for 24 h in medium with IC_{50} values of the compounds and mitoxantrone. At least 10.000 cells were analyzed per sample, and quadrant analysis was performed).

Table 3. Apoptotic rates of compounds on A549 cell lines (%).

-	Early Apoptotic Cells	Late Apoptotic Cells	Apoptotic Cells	Necrotic Cells	Viable Cells
Control	2.6	3.5	6.1	2.1	91.8
2a	5.1	2.9	8.0	1.2	90.8
2b	15.7	14.1	29.8	4.9	65.3
2i	7.7	2.7	10.4	3.7	85.9
2j	10.7	4.2	14.9	4	81.1
2k	11.5	3.6	15.1	4	80.9
2l	1.2	7.6	8.8	63.3	27.9
R.F.	27.9	0.8	28.7	0.5	70.8

R.F: Reference drug (Mitoxantrone). (A549 cells were cultured for 24 h in medium with IC_{50} values of Compounds and mitoxantrone. At least 10.000 cells were analyzed per sample, and quadrant analysis was performed.)

the best effective and its activity was more than that of mitoxantrone. After the administration of compound **2l**, the rate of the viable cell was found low, but the cell death occurred with necrosis which was undesirable. Therefore, the anticancer activity of compound **2l** was found poor. Apoptotic rates of the compounds against C6 and A549 cell lines are shown in Tables **2** and **3**.

3.3. Prediction of ADME Parameters

The number of hydrogen bond acceptor (HBA) for all molecules were stated between 2 and 5. Low hydrogen bond donor (HBD) number for all compounds was observed and was determined between 1-2. Topological polar surface areas (TPSA) were stated between 65.52 and 93.21. Log P values were found to be between 2.28 and 4.09. The water solubility of the compounds was determined to be soluble or moderately soluble. The gastrointestinal absorptions (GIA) of the compounds were found high. Compounds **2d**, **2f**, **2g**, **2h,** and **2l** could pass the blood-brain barrier (BBB). According to these results, there was no violation of Lipinski's rule of five [70]. Even if there was no exact finding in practice, these scores were in harmony with the activity potential of the compounds and these approximations would inspire drug design. Thus, it may be suggested that synthesized compounds may have a good pharmacokinetic profile. Additionally, these findings are making them potential orally bioavailable anticancer agents. All findings were shown in Table **4**.

3.4. The Molecular Docking Study

To predict the mechanism of action and to understand the structure-activity relationship (SAR), the active compounds (**2b** and **2f**) and dasatinib docked to the active site of protein kinase. The 4YBJ crystal was chosen to establish the activity

Table 4. Predictions of some physicochemical parameters of the compounds 2a-2l.

-	PP			Lipophilicity	Water Solubility	Pharmacokinetics		Druglikeness
-	HBA	HBD	TPSA	Log P	Log S-WS	GIA	BBB	n. V
2a	3	1	78.41	2.28	-3.25-soluble	High	No	0
2b	3	1	78.41	2.30	-3.46-soluble	High	No	0
2c	2	2	81.31	2.28	-3.28-soluble	High	No	0
2d	2	1	70.45	2.31	-3.31-soluble	High	Yes	0
2e	2	2	81.31	3.18	-4.28-moderately soluble	High	No	0
2f	2	1	65.52	3.98	-5.06-moderately soluble	High	Yes	0
2g	2	1	65.52	3.98	-5.06-moderately soluble	High	Yes	0
2h	2	1	68.76	3.11	-4.12-moderately soluble	High	Yes	0
2i	5	1	65.52	4.09	-4.73-moderately soluble	High	No	0
2j	3	2	85.75	2.63	-3.76-soluble	High	No	0
2k	5	1	93.21	3.01	-4.09-moderately soluble	High	No	0
2l	2	1	65.52	3.99	-4.74-moderately soluble	High	Yes	0

PP: Physicochemical Properties, HBA: Number of hydrogen acceptors, HBD: Number of hydrogen donors, TPSA: Topological polar surface area (Å²), Log P: Octanol/water partition coefficient, LogS-WS: Water Solubility, GIA: Gastrointestinal absorption, BBB: Blood-brain barrier permeability, n. V: number of violations (For Lipinski's rule of 5). All parameters were calculated by online *via* http://www.swissadme.ch/index.php.

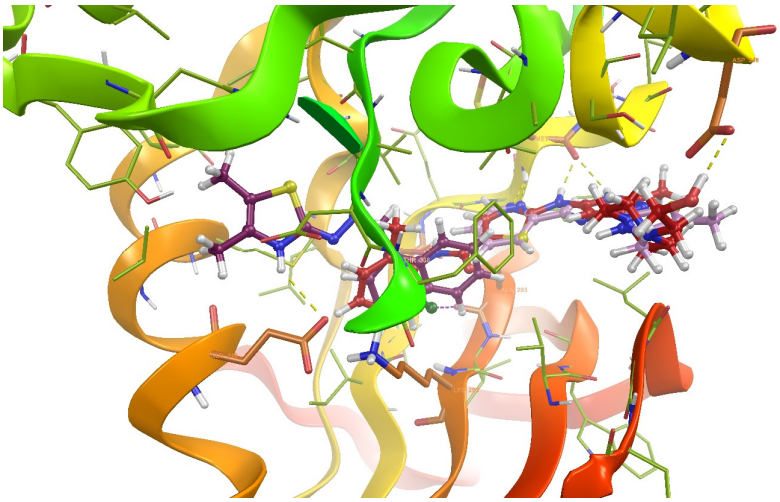

Fig. (3). Compounds **2b** (plum carbons) and **2f** (maroon carbons), and dasatinib (red carbons) in kinase active site (PDBID: 4YBJ). The active site residues were draw in stick form (yellow-green carbons). If there is an interaction between ligand and residue, these residues were represented in a ball-stick form (orange carbons). (*A higher resolution / colour version of this figure is available in the electronic copy of the article*).

mechanism and selectivity of the synthesized compounds. The 2D and 3D poses were represented in Figs. (**3-8**).

Dasatinib has three H-bonds with Met341, one H-bond with Asp348, one H-bond with Tyr338 and one halogen bond with Ala293. Compound **2b** only displayed H-bond with Met341. On the other hand, compound **2f** displayed one H-bond with Glu310 and one π -cation interaction with Met341.

4. DISCUSSION

Cancer is a complex and deadly disease. The treatment after the metastasizing is especially difficult. One of the common problems in cancer treatment is the death of cancer cells *via* necrosis. Apoptotic cell death is natural and a life-sustaining incident according to necrosis [71]. Additionally, the inhibition of the protein kinases is one of the keys of lung carcinoma and glioma treatments [72]. There are a lot of

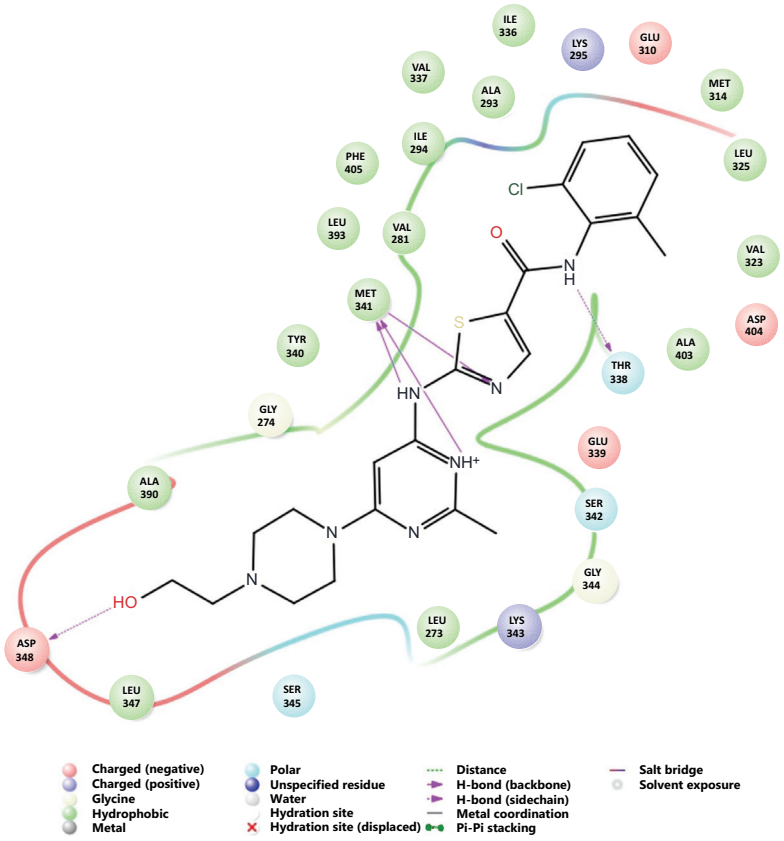

Fig. (4). 2D interaction diagram of dasatinib in active site. (PDBID: 4YBJ). (*A higher resolution / colour version of this figure is available in the electronic copy of the article*).

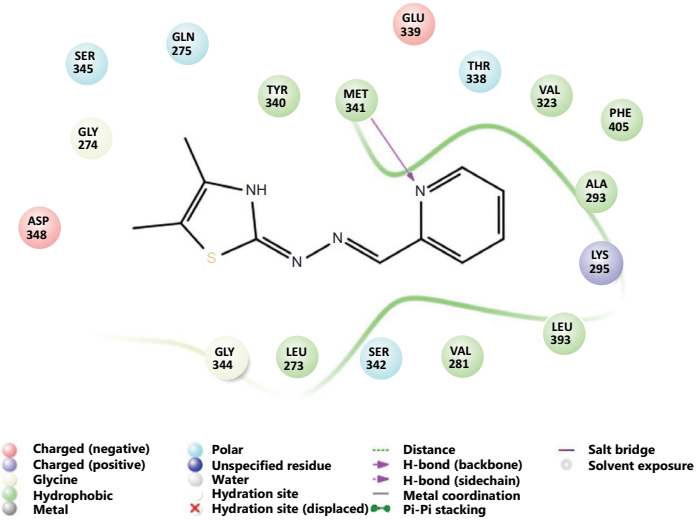

Fig. (5). 2D interaction diagram of compound **2b** in active site. (PDBID: 4YBJ). (*A higher resolution / colour version of this figure is available in the electronic copy of the article*).

studies about designing the anticancer agents that our research groups have worked on [73-76]. From the results of all these studies, we aimed to first design the final molecules that induce cell death *via* apoptosis, and then clarify the activation pathway.

In this study, the results showed that various aromatic rings bearing hydrazone linked 4,5-dimethyl thiazole have similar activity but in different potency. Pyridine-2-yl substitution on linker (hydrazone) carbon increased the activity. Our previous study [49] supported that the pyridine-2-yl (pyrimidin-2-yl as bioisosteric replacement) substitution on linker has better activity than phenyl ring. It may be caused by hydrogen bonding of the nitrogen at the active site. In fact, this H-bond was simulated *via* molecular modeling study (Fig. **5**). Although nitrogen-containing

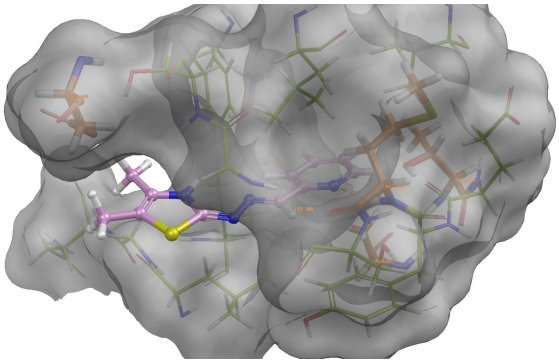

Fig. (6). Compound **2b** in active site as 3D pose. (*A higher resolution / colour version of this figure is available in the electronic copy of the article*).

aromatic structures were found more selective, except indol-3-yl, there was no harmony between bicyclic aromatics and the other aromatics. Interestingly, 4-(*N*,*N*-dimethylamino)phenyl and 3-indolyl substitutions damped down the cytotoxicity against cancer cells. Furthermore, indol-3-yl substitution did not show cytotoxic activity against any cell lines. Both situations may be caused by a lot of reasons such as solubility or failure to reach the active site. The solubility (here mean the diffusion ability), or failure to settle into the active site is the first-sight hypothesis for non-active or low potent-active compounds. The solubility is essential for diffusing into the membrane or reaching the active site. The remarkable point between compounds **2h-2l** is the electron-withdrawing substituents at ortho/para positions (**2i** and **2j**) which have more activity than the electron-donating substituents at any position (**2h**, **2k,** and **2l**) on the phenyl ring.

Compound **2b** was determined as the most selective and active compound against A549 cells. However, theoretically, compound **2b** could not pass the BBB, but compound **2f** could. Thus, it is more favorable that compound **2b** be designated for anti-adenocarcinoma and compound **2f** for anti-glioma drug investigations.

Unfortunately, the MTT studies showed modest activity. Therefore, we did not test the compounds against any enzyme. However, since they have a similar moiety to dasatinib, and we want to understand and explain the SAR better, we achieved the docking study. It provided us a new window to foresee future studies. Especially, compound **2f** could be more valuable to be designed for the inhibition of protein kinase. For **2f**, there is a potential for this compound to be a highly selective inhibitor. Since the Type II protein kinase inhibitor drugs, lapatinib, vemurafenib, and ibrutinib which are approved by FDA occupy the DFG pocket and gain selectivity because of the hydrogen bonding to Glu310 and Asp404, thus, the inhibition of these two amino acids has pharmacological importance [69]. Our docking study displayed that compound **2f** builds up one H-bond with Glu310. This interaction is not enough for the high inhibitory activity but it is important for selectivity. Besides, compound **2b** could be substituted on the pyridine ring such as dasatinib. Hereby, the activity potency could be increased. However, both compounds fit well into the active site.

Briefly, results of *in vitro* and *in silico* studies revealed that the active compounds (**2b** and **2f**) were promising agents for cancer treatment and useful as intermediates to design and to develop new molecules. Compound **2b** was determined as the most selective and active compound against A549 cells. However, theoretically, compound **2b** could not

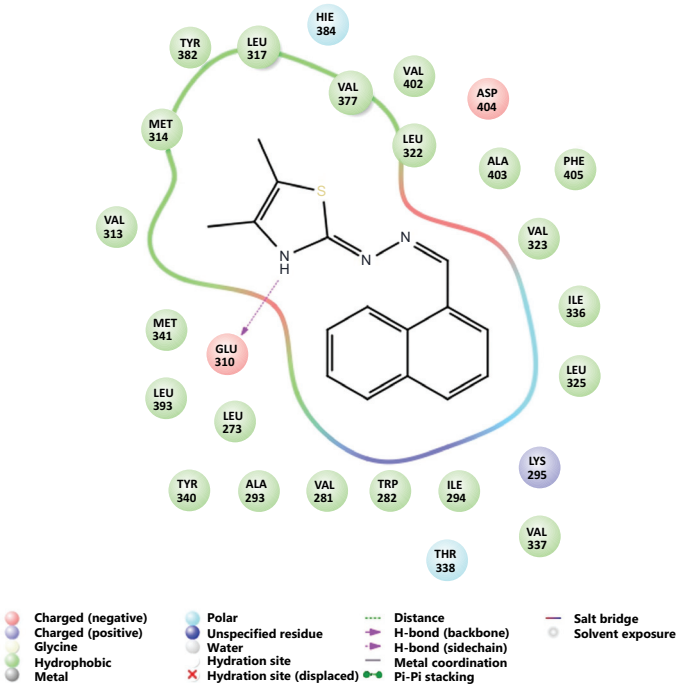

Fig. (7). 2D interaction diagram of compound **2f** in active site. (PDBID: 4YBJ). (*A higher resolution / colour version of this figure is available in the electronic copy of the article*).

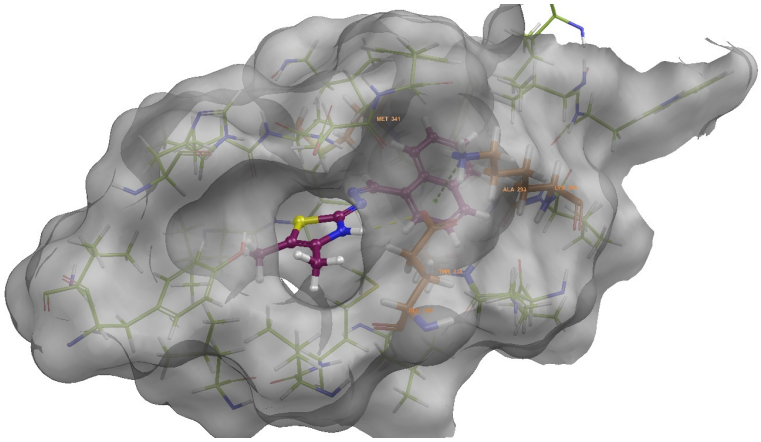

Fig. (8). Compound **2f** in active site as 3D pose. (*A higher resolution / colour version of this figure is available in the electronic copy of the article*).

pass the BBB, but compound **2f** could do. So, it is thought that compound **2b** is more favorable to be designated for anti-adenocarcinoma and compound **2f** for anti-glioma drug investigations. Due to the similarity to dasatinib, the core structures of **2b** and **2f** could be used to gain selective inhibitors of protein kinase.

CONCLUSION

In this study, we synthesized and analyzed twelve thiazole-hydrazone derivatives (**2a-2l**), and then evaluated their cytotoxicity against A549 human lung adenocarcinoma, C6 rat glioma, NIH3T3 fibroblast, and L929 fibroblast cell lines. The results showed that compound **2b** was the most active compound against A549 and C6 cells in the *in vitro* study, but it cannot pass the blood-brain barrier theoretically. Compound **2f** showed good anti-glioma activity in *in vitro* study. Consequently, compound **2f** was stated as an option to be an anticancer drug against brain tumors, and compound **2b** was determined as an alternative for the anticancer agents against lung cancer. In future studies, it will be our priority to focus on the development of derivatives of these two compounds (**2b** and **2f**) and elucidate their mechanisms.

AUTHORS' CONTRIBUTIONS

L.Y. and G.A.Ç. designed the study. A.E.E. performed the docking study. A.E.E., O.A. and B.E. did chemical and biological experiments. L.Y., A.E.E. and G.A.Ç. analyzed data and A.E.E. wrote the manuscript.

CONSENT FOR PUBLICATION

Not applicable.

AVAILABILITY OF DATA AND MATERIALS

The authors confirm that the data supporting the findings of this research are available with in the manuscript.

FUNDING

None.

CONFLICT OF INTEREST

The authors declare no conflict of interest, financial or otherwise.

ACKNOWLEDGEMENTS

We gratefully thank Anadolu University DOPNA Laboratory for analyzing the synthesized compounds.

SUPPLEMENTARY MATERIAL

Supplementary material is available on the publisher's website along with the published article.

REFERENCES

[1] Carmeliet, P.; Jain, R.K. Angiogenesis in cancer and other diseases. *Nature,* **2000**, *407*(6801), 249-257. http://dx.doi.org/10.1038/35025220 PMID: 11001068

[2] Reya, T.; Morrison, S.J.; Clarke, M.F.; Weissman, I.L. Stem cells, cancer, and cancer stem cells. *Nature,* **2001**, *414*(6859), 105-111. http://dx.doi.org/10.1038/35102167 PMID: 11689955

[3] Fitzmaurice, C.; Allen, C.; Barber, R.M.; Barregard, L.; Bhutta, Z.A.; Brenner, H.; Dicker, D.J.; Chimed-Orchir, O.; Dandona, R.; Dandona, L. Global, regional, and national cancer incidence, mortality, years of life lost, years lived with disability, and disability-adjusted life-years for 32 cancer groups, 1990 to 2015: a systematic analysis for the global burden of disease study. *JAMA Oncol.,* **2017**, *3*(4), 524-548. http://dx.doi.org/10.1001/jamaoncol.2016.5688 PMID: 27918777

[4] de Sá, V.K.; Coelho, J.C.; Capelozzi, V.L.; de Azevedo, S.J. Lung cancer in Brazil: Epidemiology and treatment challenges. *Lung Cancer (Auckl.),* **2016**, *7*, 141-148. http://dx.doi.org/10.2147/LCTT.S93604 PMID: 28210170

[5] Dela Cruz, C.S.; Tanoue, L.T.; Matthay, R.A. Lung cancer: epidemiology, etiology, and prevention. *Clin. Chest Med.,* **2011**, *32*(4), 605-644. http://dx.doi.org/10.1016/j.ccm.2011.09.001 PMID: 22054876

[6] Walker, M.D.; Alexander, E., Jr; Hunt, W.E.; MacCarty, C.S.; Mahaley, M.S., Jr; Mealey, J., Jr; Norrell, H.A.; Owens, G.; Ransohoff, J.; Wilson, C.B.; Gehan, E.A.; Strike, T.A. Evaluation of BCNU and/or radiotherapy in the treatment of anaplastic gliomas. A cooperative clinical trial. *J. Neurosurg.,* **1978**, *49*(3), 333-343. http://dx.doi.org/10.3171/jns.1978.49.3.0333 PMID: 355604

[7] Sulu, E.; Tasolar, O.; Berk Takir, H.; Yagci Tuncer, L.; Karakurt, Z.; Yilmaz, A. Delays in the diagnosis and treatment of non-small-cell lung cancer. *Tumori,* **2011**, *97*(6), 693-697. http://dx.doi.org/10.1177/030089161109700603 PMID: 22322833

[8] Wen, P.Y.; Chang, S.M.; Lamborn, K.R.; Kuhn, J.G.; Norden, A.D.; Cloughesy, T.F.; Robins, H.I.; Lieberman, F.S.; Gilbert, M.R.; Mehta, M.P.; Drappatz, J.; Groves, M.D.; Santagata, S.; Ligon, A.H.; Yung, W.K.; Wright, J.J.; Dancey, J.; Aldape, K.D.; Prados, M.D.; Ligon, K.L. Phase I/II study of erlotinib and temsirolimus for patients with recurrent malignant gliomas: North American Brain Tumor Consortium trial 04-02. *Neuro-oncol.,* **2014**, *16*(4), 567-578.
http://dx.doi.org/10.1093/neuonc/not247 PMID: 24470557

[9] Lassman, A.B.; Pugh, S.L.; Gilbert, M.R.; Aldape, K.D.; Geinoz, S.; Beumer, J.H.; Christner, S.M.; Komaki, R.; DeAngelis, L.M.; Gaur, R.; Youssef, E.; Wagner, H.; Won, M.; Mehta, M.P. Phase 2 trial of dasatinib in target-selected patients with recurrent glioblastoma (RTOG 0627). *Neuro-oncol.,* **2015**, *17*(7), 992-998.
http://dx.doi.org/10.1093/neuonc/nov011 PMID: 25758746

[10] Banerjee, A.; Jakacki, R.I.; Onar-Thomas, A.; Wu, S.; Nicolaides, T.; Young Poussaint, T.; Fangusaro, J.; Phillips, J.; Perry, A.; Turner, D.; Prados, M.; Packer, R.J.; Qaddoumi, I.; Gururangan, S.; Pollack, I.F.; Goldman, S.; Doyle, L.A.; Stewart, C.F.; Boyett, J.M.; Kun, L.E.; Fouladi, M. A phase I trial of the MEK inhibitor selumetinib (AZD6244) in pediatric patients with recurrent or refractory low-grade glioma: a pediatric brain Tumor Consortium (PBTC) study. *Neuro-oncol.,* **2017**, *19*(8), 1135-1144.
http://dx.doi.org/10.1093/neuonc/now282 PMID: 28339824

[11] Helal, M.H.; El-Awdan, S.A.; Salem, M.A.; Abd-elaziz, T.A.; Moahamed, Y.A.; El-Sherif, A.A.; Mohamed, G.A. Synthesis, biological evaluation and molecular modeling of novel series of pyridine derivatives as anticancer, anti-inflammatory and analgesic agents. *Spectrochim. Acta A Mol. Biomol. Spectrosc.,* **2015**, *135*, 764-773.
http://dx.doi.org/10.1016/j.saa.2014.06.145 PMID: 25150427

[12] Carbone, A.; Pennati, M.; Parrino, B.; Lopergolo, A.; Barraja, P.; Montalbano, A.; Spanò, V.; Sbarra, S.; Doldi, V.; De Cesare, M.; Cirrincione, G.; Diana, P.; Zaffaroni, N. Novel 1H-pyrrolo[2,3-b]pyridine derivative nortopsentin analogues: Synthesis and antitumor activity in peritoneal mesothelioma experimental models. *J. Med. Chem.,* **2013**, *56*(17), 7060-7072.
http://dx.doi.org/10.1021/jm400842x PMID: 23919303

[13] Jones, V.S.; Huang, R.Y.; Chen, L.P.; Chen, Z.S.; Fu, L.; Huang, R.P. Cytokines in cancer drug resistance: Cues to new therapeutic strategies. *Biochim. Biophys. Acta,* **2016**, *1865*(2), 255-265.
PMID: 26993403

[14] Salgia, R.; Kulkarni, P. The genetic/non-genetic duality of drug 'resistance' in cancer. *Trends Cancer,* **2018**, *4*(2), 110-118.
http://dx.doi.org/10.1016/j.trecan.2018.01.001 PMID: 29458961

[15] Siegfried, Z.; Karni, R. The role of alternative splicing in cancer drug resistance. *Curr. Opin. Genet. Dev.,* **2018**, *48*, 16-21.
http://dx.doi.org/10.1016/j.gde.2017.10.001 PMID: 29080552

[16] Franceschini, G.; Martin Sanchez, A.; Di Leone, A.; Magno, S.; Moschella, F.; Accetta, C.; Masetti, R. New trends in breast cancer surgery: A therapeutic approach increasingly efficacy and respectful of the patient. *G. Chir.,* **2015**, *36*(4), 145-152.
PMID: 26712068

[17] Eberli, D.; Mortezavi, A.; Sulser, T. Focal therapy-a new era in the treatment of prostate cancer. Praxis (Bern 1994), **2014**, 103, pp. (7)391-397.

[18] Salama, J.K.; Vokes, E.E. New radiotherapy and chemoradiotherapy approaches for non-small-cell lung cancer. *J. Clin. Oncol.,* **2013**, *31*(8), 1029-1038.
http://dx.doi.org/10.1200/JCO.2012.44.5064 PMID: 23401449

[19] Yurttas, L.; Ozkay, Y.; Akalin, G.; Ulusoylar, Yildirim Synthesis and anticancer activity evaluation of N-[4-(2-methylthiazol-4-yl)phenyl]acetamide derivatives containing (benz)azole moiety. *J. Enzyme Inhib. Med. Chem.,* **2014**, *29*(2), 175-184.
http://dx.doi.org/10.3109/14756366.2013.763253 PMID: 23391122

[20] Vashist, S.K.; Luppa, P.B.; Yeo, L.Y.; Ozcan, A.; Luong, J.H.T. Emerging technologies for next-generation point-of-care testing. *trends Biotechnol.,* **2015**, *33*(11), 692-705.
http://dx.doi.org/10.1016/j.tibtech.2015.09.001 PMID: 26463722

[21] Porcari, P.; Hegi, M.E.; Lei, H.; Hamou, M.F.; Vassallo, I.; Capuani, S.; Gruetter, R.; Mlynarik, V. Early detection of human glioma sphere xenografts in mouse brain using diffusion MRI at 14.1 T. *NMR Biomed.,* **2016**, *29*(11), 1577-1589.
http://dx.doi.org/10.1002/nbm.3610 PMID: 27717037

[22] van Dijken, B.R.J.; van Laar, P.J.; Holtman, G.A.; van der Hoorn, A. Diagnostic accuracy of magnetic resonance imaging techniques for treatment response evaluation in patients with high-grade glioma, a systematic review and meta-analysis. *Eur. Radiol.,* **2017**, *27*(10), 4129-4144.
http://dx.doi.org/10.1007/s00330-017-4789-9 PMID: 28332014

[23] Cai, S.X.; Nguyen, B.; Jia, S.; Herich, J.; Guastella, J.; Reddy, S.; Tseng, B.; Drewe, J.; Kasibhatla, S. Discovery of substituted N-phenyl nicotinamides as potent inducers of apoptosis using a cell- and caspase-based high throughput screening assay. *J. Med. Chem.,* **2003**, *46*(12), 2474-2481.
http://dx.doi.org/10.1021/jm0205200 PMID: 12773051

[24] Yurttas, L.; Demir, B.; Ciftci, G.A. Some Thiazole Derivatives Combined With Different Heterocycles : Cytotoxicity Evaluation And Apoptosis Inducing StudiesAnti-Cancer Agent Me, **2018**.

[25] Altintop, M.D.; Sever, B.; Akalin, G.; Turan-Zitouni, G.; Kaplancikli,, Z.A.; Ozdemir, A. Design, synthesis, in vitro and in silico evaluation of a new series of oxadiazole-based anticancer agents as potential Akt and FAK inhibitors. *Eur. J. Med. Chem.,* **2018**, *155*, 905-924.
http://dx.doi.org/10.1016/j.ejmech.2018.06.049 PMID: 29966916

[26] Asati, V.; Mahapatra, D.K.; Bharti, S.K. Thiazolidine-2,4-diones as multi-targeted scaffold in medicinal chemistry: Potential anticancer agents. *Eur. J. Med. Chem.,* **2014**, *87*, 814-833.
http://dx.doi.org/10.1016/j.ejmech.2014.10.025 PMID: 25440883

[27] Creelan, B.C.; Antonia, S.J. Immunotherapy in lung cancer: "b7-bombers" and other new developments. *Semin. Respir. Crit. Care Med.,* **2013**, *34*(6), 810-821.
http://dx.doi.org/10.1055/s-0033-1358551 PMID: 24258571

[28] Rouf, A.; Tanyeli, C. Bioactive thiazole and benzothiazole derivatives. *Eur. J. Med. Chem.,* **2015**, *97*, 911-927.
http://dx.doi.org/10.1016/j.ejmech.2014.10.058 PMID: 25455640

[29] Al-Saadi, M.S.; Faidallah, H.M.; Rostom, S.A. Synthesis and biological evaluation of some 2,4,5-trisubstituted thiazole derivatives as potential antimicrobial and anticancer agents. *Arch. Pharm. (Weinheim),* **2008**, *341*(7), 424-434.
http://dx.doi.org/10.1002/ardp.200800026 PMID: 18574850

[30] Tsuno, N.; Yukimasa, A.; Yoshida, O.; Ichihashi, Y.; Inoue, T.; Ueno, T.; Yamaguchi, H.; Matsuda, H.; Funaki, S.; Yamanada, N.; Tanimura, M.; Nagamatsu, D.; Nishimura, Y.; Ito, T.; Soga, M.; Horita, N.; Yamamoto, M.; Hinata, M.; Imai, M.; Morioka, Y.; Kanemasa, T.; Sakaguchi, G.; Iso, Y. Discovery of novel 2′,4′-dimethyl-[4,5′-bithiazol]-2-yl amino derivatives as orally bioavailable TRPV4 antagonists for the treatment of pain: Part 1. *Bioorg. Med. Chem. Lett.,* **2016**, *26*(20), 4930-4935.
http://dx.doi.org/10.1016/j.bmcl.2016.09.013 PMID: 27637151

[31] Chandak, N.; Kumar, P.; Kaushik, P.; Varshney, P.; Sharma, C.; Kaushik, D.; Jain, S.; Aneja, K.R.; Sharma, P.K. Dual evaluation of some novel 2-amino-substituted coumarinylthiazoles as anti-inflammatory-antimicrobial agents and their docking studies with COX-1/COX-2 active sites. *J. Enzyme Inhib. Med. Chem.,* **2014**, *29*(4), 476-484.
http://dx.doi.org/10.3109/14756366.2013.805755 PMID: 23777557

[32] Albuquerque, J.F.; Albuquerque, A.; Azevedo, C.C.; Thomasson, F.; Galdino, L.S.; Chantegrel, J.; Catanho, M.T.; Pitta, I.R.; Luu-Duc, C. Substituted thiazolidinediones and thio-imidazolidinones: Synthesis, structural study and pharmacological activity. *Pharmazie,* **1995**, *50*(6), 387-389.
PMID: 7651975

[33] Akalin Ciftci, G.; Altıntop, M.D.; Edip Temel, H.; Ozdemir, A.; Kaplancıklı, Z.A. Cytotoxic, apoptotic and DNA synthesis inhibitory effects of some thiazole derivatives. *Lett. Drug Des. Discov.,* **2017**, *14*(5), 554-566.
http://dx.doi.org/10.2174/1570180813666160907170553

[34] Yahya, S.M.M.; Abdelhamid, A.O.; Abd-Elhalim, M.M.; Elsayed, G.H.; Eskander, E.F. The effect of newly synthesized progesterone derivatives on apoptotic and angiogenic pathway in MCF-7 breast cancer cells. *Steroids,* **2017**, *126*, 15-23.
http://dx.doi.org/10.1016/j.steroids.2017.08.002 PMID: 28797724

[35] Saha, S.; Chan, D.S.; Lee, C.Y.; Wong, W.; New, L.S.; Chui, W.K.; Yap, C.W.; Chan, E.C.; Ho, H.K. Pyrrolidinediones reduce the toxicity of thiazolidinediones and modify their anti-diabetic and anti-cancer properties. *Eur. J. Pharmacol.,* **2012**, *697*(1-3), 13-23.
http://dx.doi.org/10.1016/j.ejphar.2012.09.021 PMID: 23041271

[36] Weber, G.; Nagai, M.; Natsumeda, Y.; Eble, J.N.; Jayaram, H.N.; Paulik, E.; Zhen, W.N.; Hoffman, R.; Tricot, G. Tiazofurin down-regulates expression of c-Ki-ras oncogene in a leukemic patient. *Cancer Commun.,* **1991**, *3*(3), 61-66.

http://dx.doi.org/10.3727/095535491820873579 PMID: 1705812

[37] Patay, Z.; Merchant, T.E.; Nguyen, R.; Pierson, C.R.; Onar-Thomas, A.; Broniscer, A. Treatment-related noncontiguous radiologic changes in children with diffuse intrinsic pontine glioma treated with expanded irradiation fields and antiangiogenic therapy. *Int. J. Radiat. Oncol. Biol. Phys.,* **2017**, *99*(5), 1295-1305. http://dx.doi.org/10.1016/j.ijrobp.2017.08.021 PMID: 29165288

[38] Broniscer, A.; Baker, S.D.; Wetmore, C.; Pai Panandiker, A.S.; Huang, J.; Davidoff, A.M.; Onar-Thomas, A.; Panetta, J.C.; Chin, T.K.; Merchant, T.E.; Baker, J.N.; Kaste, S.C.; Gajjar, A.; Stewart, C.F. Phase I trial, pharmacokinetics, and pharmacodynamics of vandetanib and dasatinib in children with newly diagnosed diffuse intrinsic pontine glioma. *Clin. Cancer Res.,* **2013**, *19*(11), 3050-3058. http://dx.doi.org/10.1158/1078-0432.CCR-13-0306 PMID: 23536435

[39] Narang, R.; Narasimhan, B.; Sharma, S. A review on biological activities and chemical synthesis of hydrazide derivatives. *Curr. Med. Chem.,* **2012**, *19*(4), 569-612. http://dx.doi.org/10.2174/092986712798918789 PMID: 22204327

[40] Carradori, S.; Rotili, D.; De Monte, C.; Lenoci, A.; D'Ascenzio, M.; Rodriguez, V.; Filetici, P.; Miceli, M.; Nebbioso, A.; Altucci, L.; Secci, D.; Mai, A. Evaluation of a large library of (thiazol-2-yl)hydrazones and analogues as histone acetyltransferase inhibitors: Enzyme and cellular studies. *Eur. J. Med. Chem.,* **2014**, *80*, 569-578. http://dx.doi.org/10.1016/j.ejmech.2014.04.042 PMID: 24835815

[41] Domagala, A.; Jarosz, T.; Lapkowski, M. Living on pyrrolic foundations - advances in natural and artificial bioactive pyrrole derivatives. *Eur. J. Med. Chem.,* **2015**, *100*, 176-187. http://dx.doi.org/10.1016/j.ejmech.2015.06.009 PMID: 26087028

[42] De Coen, L.M.; Heugebaert, T.S.; García, D.; Stevens, C.V. Synthetic entries to and biological activity of pyrrolopyrimidines. *Chem. Rev.,* **2016**, *116*(1), 80-139. http://dx.doi.org/10.1021/acs.chemrev.5b00483 PMID: 26699634

[43] Garuti, L.; Roberti, M.; Pizzirani, D. Nitrogen-containing heterocyclic quinones: A class of potential selective antitumor agents. *Mini Rev. Med. Chem.,* **2007**, *7*(5), 481-489. http://dx.doi.org/10.2174/138955707780619626 PMID: 17504183

[44] Novak, R.F.; Kaul, K.L.; Kim, S.G. Induction of the alcohol-inducible form of cytochrome P-450 by nitrogen-containing heterocycles: Effects on pyridine N-oxide production. *Drug Metab. Rev.,* **1989**, *20*(2-4), 781-792. http://dx.doi.org/10.3109/03602538909103578 PMID: 2680407

[45] Clézardin, P.; Massaia, M. Nitrogen-containing bisphosphonates and cancer immunotherapy. *Curr. Pharm. Des.,* **2010**, *16*(27), 3007-2014. http://dx.doi.org/10.2174/138161210793563545 PMID: 20722623

[46] Işık, S.; Vullo, D.; Durdagi, S.; Ekinci, D.; Şentürk, M.; Çetin, A.; Şentürk, E.; Supuran, C.T. Interaction of carbonic anhydrase isozymes I, II, and IX with some pyridine and phenol hydrazinecarbothioamide derivatives. *Bioorg. Med. Chem. Lett.,* **2015**, *25*(23), 5636-5641. http://dx.doi.org/10.1016/j.bmcl.2015.10.021 PMID: 26520662

[47] Abd El-All, A.S.; Osman, S.A.; Roaiah, H.M.F.; Abdalla, M.M.; Abd El Aty, A.A. AbdEl-Hady, W.H., Potent anticancer and antimicrobial activities of pyrazole, oxazole and pyridine derivatives containing 1,2,4-triazine moiety. *Med. Chem. Res.,* **2015**, *24*(12), 4093-4104. http://dx.doi.org/10.1007/s00044-015-1460-3

[48] Secci, D.; Bizzarri, B.; Bolasco, A.; Carradori, S.; D'Ascenzio, M.; Rivanera, D.; Mari, E.; Polletta, L.; Zicari, A. Synthesis, anti-Candida activity, and cytotoxicity of new (4-(4-iodophenyl)thiazol-2-yl)hydrazine derivatives. *Eur. J. Med. Chem.,* **2012**, *53*, 246-253. http://dx.doi.org/10.1016/j.ejmech.2012.04.006 PMID: 22560629

[49] Evren, A.E.; Yurttaş, L.; Ekselli, B.; Akalın-Cıftcı, G. Novel Tri-substituted Thiazoles Bearing Piperazine Ring: Synthesis and evaluation of their anticancer activity. *Lett. Drug Des. Discov.,* **2019**, *16*(5), 547-555. http://dx.doi.org/10.2174/1570180815666180731122118

[50] Grunberg, E.; Leiwant, B. Antitubercular activity *in vivo* of nicotinaldehyde thiosemicarbazone and its isomers. *Exp. Biol. Med.,* **1951**, *77*(1), 47-50. http://dx.doi.org/10.3181/00379727-77-18673 PMID: 14844390

[51] Anderson, F.E.; Duca, C.J.; Scudi, J.V. Some heterocyclic thiosemicarbazones. *J. Am. Chem. Soc.,* **1951**, *73*(10), 4967-4968. http://dx.doi.org/10.1021/ja01154a501

[52] Yurttaş, L.; Özkay, Y.; Kaplancıklı, Z.A.; Tunalı, Y.; Karaca, H. Synthesis and antimicrobial activity of some new hydrazone-bridged thiazole-pyrrole derivatives. *J. Enzyme Inhib. Med. Chem.,* **2013**, *28*(4), 830-835. http://dx.doi.org/10.3109/14756366.2012.688043 PMID: 22651798

[53] Weller, L.E.; Sell, H.M.; Gottshall, R.Y. 3-Indolecarboxaldehyde thiosemicarbazone, a new antitubercular compound1. *J. Am. Chem. Soc.,* **1954**, *76*(7), 1959-1959. http://dx.doi.org/10.1021/ja01636a075

[54] Bernstein, J.; Yale, H.L.; Losee, K.; Holsing, M.; Martins, J.; Lott, W.A. The Chemotherapy of experimental tuberculosis. iii. the synthesis of thiosemicarbazones and related compounds1,2. *J. Am. Chem. Soc.,* **1951**, *73*(3), 906-912. http://dx.doi.org/10.1021/ja01147a007

[55] Jensen, K.A.; Jensen, C.L.; Frank, A.; Harvey, W.E.; Östling, S. Thiohydrazides and thiohydrazones: A new class of antibacterial substances. *Acta Chem. Scand.,* **1952**, *6*, 957-958. http://dx.doi.org/10.3891/acta.chem.scand.06-0957

[56] Puetzer, B.; Hamlin, W.E.; Katz, L. A Preparative method for thiosemicarbazones of aromatic aldehydes1. *J. Am. Chem. Soc.,* **1951**, *73*(6), 2958-2958. http://dx.doi.org/10.1021/ja01150a527

[57] Pignatello, R.; Mazzone, S.; Castelli, F.; Mazzone, P.; Raciti, G.; Mazzone, G. MAOI activity of thiosemicarbazides and related 2-thiazolylhydrazines. *Pharmazie,* **1994**, *49*(4), 272-276. PMID: 8197227

[58] Goldfarb, D.S. Method for altering the lifespan of eukaryotic organisms. US 8,642,660 B2, **2014**.

[59] Turan-Zitouni, G.; Altintop, M.D.; Ozdemir, A.; Kaplancikli, Z.A.; Kaplancikli, G.A.; Temel, H.E. Synthesis and evaluation of bis-thiazole derivatives as new anticancer agents. *Eur. J. Med. Chem.,* **2016**, *107*, 288-294. http://dx.doi.org/10.1016/j.ejmech.2015.11.002 PMID: 26599534

[60] Bahuguna, A.; Khan, I.; Bajpai, V.K.; Kang, S.C. S.C. MTT assay to evaluate the cytotoxic potential of a drug. *Bangl. J. Pharmacol,* **2017**, *12*(2), doi:10.3329/bjp.v12i2.30892.

[61] Eldeniz, A.U.; Mustafa, K.; Orstavik, D.; Dahl, J.E. Cytotoxicity of new resin-, calcium hydroxide- and silicone-based root canal sealers on fibroblasts derived from human gingiva and L929 cell lines. *Int. Endod. J.,* **2007**, *40*(5), 329-337. http://dx.doi.org/10.1111/j.1365-2591.2007.01211.x PMID: 17309743

[62] Theiszová, M.; Jantova, S.; Dragunova, J.; Grznarova, P.; Palou, M. Comparison the cytotoxicity of hydroxyapatite measured by direct cell counting and MTT test in murine fibroblast NIH-3T3 cells. *Biomedical Papers,* **2005**, *149*(2), 393-396. http://dx.doi.org/10.5507/bp.2005.066 PMID: 16601796

[63] Mosmann, T. Rapid colorimetric assay for cellular growth and survival: application to proliferation and cytotoxicity assays. *J. Immunol. Methods,* **1983**, *65*(1-2), 55-63. http://dx.doi.org/10.1016/0022-1759(83)90303-4 PMID: 6606682

[64] Keiser, K.; Johnson, C.C.; Tipton, D.A. Cytotoxicity of mineral trioxide aggregate using human periodontal ligament fibroblasts. *J. Endod.,* **2000**, *26*(5), 288-291. http://dx.doi.org/10.1097/00004770-200005000-00010 PMID: 11199738

[65] Daina, A.; Michielin, O.; Zoete, V. SwissADME: a free web tool to evaluate pharmacokinetics, drug-likeness and medicinal chemistry friendliness of small molecules. *Sci. Rep.,* **2017**, *7*, 42717. http://dx.doi.org/10.1038/srep42717 PMID: 28256516

[66] Daina, A.; Michielin, O.; Zoete, V. iLOGP: a simple, robust, and efficient description of n-octanol/water partition coefficient for drug design using the GB/SA approach. *J. Chem. Inf. Model.,* **2014**, *54*(12), 3284-3301. http://dx.doi.org/10.1021/ci500467k PMID: 25382374

[67] Daina, A.; Zoete, V. A boiled-egg to predict gastrointestinal absorption and brain penetration of small molecules. *ChemMedChem,* **2016**, *11*(11), 1117-1121. http://dx.doi.org/10.1002/cmdc.201600182 PMID: 27218427

[68] Maestro, S. *Version 10.6,* **2016**.

[69] Kwarcinski, F.E.; Brandvold, K.R.; Phadke, S.; Beleh, O.M.; Johnson, T.K.; Meagher, J.L.; Seeliger, M.A.; Stuckey, J.A.; Soellner, M.B. Conformation-selective analogues of dasatinib

reveal insight into kinase inhibitor binding and selectivity. *ACS Chem. Biol.,* **2016**, *11*(5), 1296-1304.
http://dx.doi.org/10.1021/acschembio.5b01018 PMID: 26895387

[70] Lipinski, C.A.; Lombardo, F.; Dominy, B.W.; Feeney, P.J. Experimental and computational approaches to estimate solubility and permeability in drug discovery and development settings. *Adv. Drug Deliv. Rev.,* **2001**, *46*(1-3), 3-26.
http://dx.doi.org/10.1016/S0169-409X(00)00129-0
PMID: 11259830

[71] Elmore, S. Apoptosis: A review of programmed cell death. *Toxicol. Pathol.,* **2007**, *35*(4), 495-516.
http://dx.doi.org/10.1080/01926230701320337 PMID: 17562483

[72] Zhang, Z-H.; Wu, H-M.; Deng, S-N.; Chai, R-X.; Mwenda, M.C.; Peng, Y-Y.; Cai, D.; Chen, Y. Synthesis and biological evaluation of 2,4-disubstituted thiazole amide derivatives as anticancer agent. *Chem. Pap.,* **2018**, *73*(2), 355-364.
http://dx.doi.org/10.1007/s11696-018-0587-3

[73] Demirayak, S.; Yurttas, L.; Gundogdu-Karaburun, N.; Karaburun, A.C.; Kayagil, I. Synthesis and anti-cancer activity evaluation of new aurone derivatives. *J. Enzyme Inhib. Med. Chem.,* **2015**, *30*(5), 816-825.
http://dx.doi.org/10.3109/14756366.2014.976568 PMID: 25716125

[74] Evren, A.E.; Yurttas, L.; Ekselli, B.; Akalin-Ciftci, G. Synthesis and biological evaluation of 5-methyl-4-phenyl thiazole derivatives as anticancer agents. *Phosphorus Sulfur,* **2019**, *194*(8), 820-828.
http://dx.doi.org/10.1080/10426507.2018.1550642

[75] Turan-Zitouni, G.; Yurtta, L.; Tabbi, A.; Akalin, G.; Temel, H.E.; Kaplancikli, Z.A. New thiazoline-tetralin derivatives and biological activity evaluation. *Mol.,* **2018**, *23*(1), E135.
http://dx.doi.org/10.3390/molecules23010135 PMID: 29320423

[76] Saglik, B.N.; Sen, A.M.; Evren, A.E.; Cevik, U.A.; Osmaniye, D.; Kaya Cavusoglu, B.; Levent, S.; Karaduman, A.B.; Ozkay, Y.; Kaplancikli, Z.A. Synthesis, investigation of biological effects and *in silico* studies of new benzimidazole derivatives as aromatase inhibitors. *Z Naturforsch C J. Biosci.*, **2020**, *75*(9-10), 353-362.